Pearl E. Donohoo grew up in Cuyahoga Falls, Ohio. She earned a Bachelors of Science in mechanical engineering from the Franklin W. Olin College of Engineering where she was a member of the second graduating class. During her undergraduate career, she held two SULI internships at the National Renewable Energy Laboratory over the summers of 2006 and 2007. Pearl is currently a Masters student in the Technology and Policy Program at the Massachusetts Institute of Technology where she is researching alternative aviation fuels. She enjoys urban cafes and is a keen outdoorswoman.

Jason Cotrell is a Senior Project Leader at the National Renewable Energy Laboratory's National Wind Technology Center (NWTC). During his 11 year tenure at the NWTC, he has researched wind turbine drivetrains, advanced wind turbine rotors, wind-to-hydrogen systems, and equipment for wind turbine blade testing. His present focus is leading the effort to develop large blade testing facilities to be built in Massachusetts and Texas. Prior to the NWTC he obtained a BSME and MSME at UT Austin in 1995 and 1997.

Characterization of a Mobile Oscillatory Fatigue Operator for Wind Turbine Blade Testing

Pearl E. Donohoo and Jason Cotrell

ABSTRACT

Laboratory testing of wind turbine blades is required to meet wind turbine design standards, reduce machine cost, and reduce the technical and financial risks of deploying mass-produced wind turbine models. Fatigue testing at the National Wind Technology Center (NWTC) is currently conducted using Universal Resonance Excitation (UREX) technology. In a UREX test, the blade is mounted to a rigid stand and hydraulic exciters mounted to the blade are used to excite the blade to its resonant frequency. A drawback to UREX technology is that mounting hydraulic systems to the blade is difficult and requires a relatively long set-up period. An alternative testing technology called the Mobile Oscillatory Fatigue Operator (MOFO) has been analyzed. The MOFO uses an oscillating blade test-stand rather than a rigid stand, avoiding the need to place hydraulic systems on the blade. The MOFO will be demonstrated by converting an existing test-stand at the NWTC to an oscillating stand that can test blades up to 25 m in length. To obtain the loads necessary to design the MOFO, the system motion is modeled using rigid body and lumped mass dynamics models. Preliminary modeling indicates the existing stand can be converted to a MOFO relatively easily. However, the blade dynamic models suggest that blade bending moment distributions are significantly different for UREX and MOFO testing; more sophisticated models are required to assess the implication of this difference on the accuracy of the test.

Introduction

Over their lifetimes, wind turbine blades are exposed to uneven loadings. These result from varying wind distributions and uneven loading across the blade itself. Repetitive loading cycles stress blade materials and can cause failure. To certify that blades can withstand the forces and to test new blade concepts, they are first subjected to controlled fatigue and static tests. During fatigue testing, blades are preloaded with masses. They are then oscillated, both flapwise and edgewise, through approximately one million cycles to simulate field operating conditions. Testing is performed at the resonant frequency to minimize the input energy required by the test. The amplitude of oscillations is chosen to achieve a strain distribution in the blade required to accelerate conditions experienced in the field.

Symbology

θ_{b0}:	Initial angle to the center of gravity of the blade from the horizontal
θ_b:	Perturbation from θ_{b0}
θ_{ts0}:	Initial angle to the center of gravity of the test stand from the horizontal
θ_{ts}:	Perturbation from θ_{b0}
θ_h:	Angle from the horizontal to the actuator attachment point
m_b:	Mass of blade and added weights
m_{ts}:	Test stand mass
I_{ts}:	Test stand rotational moment of inertia about pivot
I_b:	Blade rotational moment of inertia about pivot
F_h:	Actuator force
k:	Spring constant of blade
ζ:	Damping ratio
c:	Damping coefficient

Fatigue testing is currently conducted at the National Renewable Energy Laboratory's National Wind Technology Center (NREL NTWC) using blade mounted testing apparatus (UREX); however, several sizes of UREX are required to accommodate a full range of blade sizes. The size of the UREX is limited by the weight it adds to the blade. Additionally, the hydraulic actuators require 3,000 psi fluid lines which travel with the UREX on the blade. The constant motion of the lines can cause leaks which require time to repair and are a safety hazard.

An oscillating test-stand would provide a universal testing mechanism, eliminate the need for moving hydraulic lines, and minimize the amount of setup time required. In addition, an oscillating stand could be used as a rigid stand for UREX testing by locking out the rotating degree of freedom. This paper explores the possibility of oscillating a current NWTC test-stand, here titled the Mobile Oscillatory Fatigue Operator (MOFO), to replace the blade mounted UREX apparatuses (Figure 1). To be a successful replacement, the MOFO must be able to generate testing loads and displacements

at the natural frequency of wind-turbine blades, and these loads must be generated with standard hydraulics. This paper discusses two dynamic models of the NWTC test-stand, their results, and preliminary design and component selection.

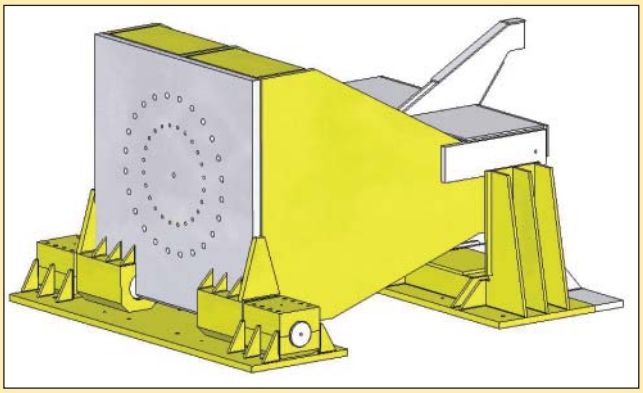

Figure 1. Model of existing NWTC test-stand.

Methods

Dynamic Load Models

Rigid body and lumped mass models were considered to determine the dynamic loading of the system at the hydraulic attachment point (Figure 2). In each model, the blade moment of inertia was calculated about the pivot point (A), the hydraulic force was constrained to act only in the vertical direction, and θ_{ts} and θ_b were decomposed into an initial angle (θ_{x0}) and a perturbation (θ_x).

Rigid Body Model

The rigid body model was analyzed first due to its simplicity. It is a single degree of freedom system with a forced angular displacement. In the rigid body model, the elasticity of the blade is assumed to be infinite such that perturbations of the blade and test-stand are equal. The perturbations (θ) are driven at a given amplitude (B) and the natural frequency of the blade (ω, Equation 1). The unknown term in Equation 1 is the hydraulic force (F_h), and time is the independent variable. The first two terms represent the moments due to the gravitational force on the blade and test stand. The second two terms represent moments due to the rotational inertias. The derivation of the equation of motion is found in Appendix A1.

$$\theta = B\sin(\omega t)$$
$$F_h(t) = \frac{-1}{l_h \cos(\theta_{h0})}\left(m_b g l_b \cos(\theta_{b0} - \theta) - m_{ts} g l_{ts} \cos(\theta_{ts0} + \theta) + \ddot{\theta} I_b + \ddot{\theta} I_{ts}\right)$$

Equation 1: Rigid body governing equation of motion.

Elastic Lumped-Mass Model

The more complicated lumped mass model was analyzed to determine how blade elasticity affects the system. The lumped mass model is a base excitation model with two degrees of freedom. It assumes the same perturbations as the rigid body model; however, it incorporates viscous damping and a torsion spring located at the pivot point to model the blade's elasticity (Equation 2). The derivation of the equation of motion is found in Appendix A2. As in Equation 1, the unknown term is the hydraulic force (F_h), and time is the independent variable. The additional fifth and sixth terms in the equation of motion represent the elasticity of the blade and aerodynamic viscous damping.

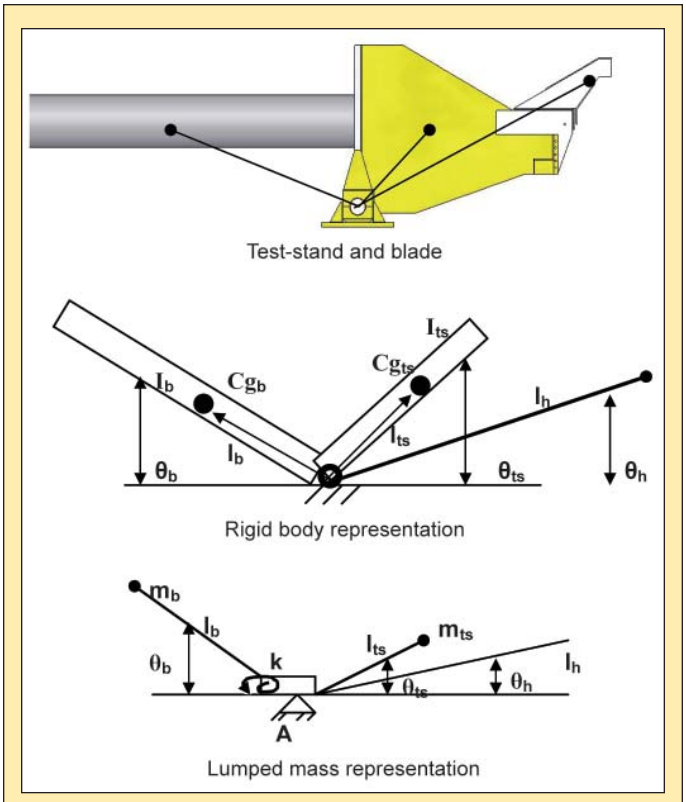

Figure 2. Test-stand model idealizations and free body diagram.

$$F_h(t) = \frac{-1}{l_h \cos\theta_{h0}}\left(m_b g l_b \cos(\theta_{b0} + \theta_b) - \ddot{\theta}_b I_b - m_{ts} g l_{ts} \cos(\theta_{ts0} + \theta_{ts})\right.$$
$$\left. + \ddot{\theta}_{ts} I_{ts} - k(\theta_b - \theta_{ts}) - c(\dot{\theta}_b - \dot{\theta}_{ts})\right)$$

Equation 2: Lumped mass governing equation of motion

With the addition of the torsion spring, the amplitude and phase of motion of the test-stand are no longer equal. The hydraulic driving function and blade response functions are determined by solving the corresponding base excitation differential equation at the blade's natural frequency (Equation 3).

$$\theta_b = B\cos\left(\omega t - \frac{\pi}{2} - \arctan\left(\frac{1}{2\varsigma}\right)\right)$$
$$\theta_h = \theta_{ts} = B\sqrt{\frac{1+(2\varsigma)^2}{(2\varsigma)^2}}^{-1}\sin(\omega t)$$

Equation 3: Base excitation response and input functions

Stand Design Considerations

Loads

Model Inputs

The model is used to calculate forces for the worst case scenario, a hypothetical 25 m blade and a 9 m experimental blade (TX) currently being tested at the NWTC. The characteristic blade constants are derived from generalized equations and from past experience with blade testing (Table 1). Constants for the 9 m blade are drawn from current fatigue testing when available. In both cases a conservative 2% viscous damping ratio is used. The effective torsion spring constant, k, is determined by assuming the blade has constant mass and stiffness matrices. Using known natural frequency values and computed rotational inertia values, the spring constant is calculated using Equation 4. The rotational moment of inertia, center of gravity, and mass of the test-stand were determined using the SolidWorks model of the stand.

$$k = \omega^2 I$$

Equation 4: Definition of spring constant value.

Model Constants					
9 m				25 m	
m_b	(kg)	454	[1]	5440	[1]
m_{ts}	(kg)	4400	[2]	4400	[2]
r_b	(m)	2.4	[3]	8.2	[4]
r_{ts}	(m)	1.1	[2]	1.1	[2]
r_h	(m)	3.2	[2]	3.2	[2]
ω	(Hz)	1.2	[3]	1	[1]
I_b	(kg m^2)	7.5e3	[5]	6.5e7	[5]
I_{ts}	(kg m^2)	8590	[2]	8590	[2]
θ_b	(rad)	±0.035	[1]	±0.035	[1]
k	(Nm)	11e3	[6]	4.2e15	[6]
ζ	(Nms^2)	0.02	[1]	0.02	[1]
c	(Nms)	0.048	[7]	0.040	[7]

[1] NWTC Estimate from current blades
[2] Measured from SolidWorks model of test-stand
[3] Measured from current blade fatigue test
[4] r_b=0.327(blade length), W. Musial and D. White, *Final Report for Large Blade Test Facility Scaling Study*. August 9, 2004.
[5] $I=(1/12)m(\text{blade length})^2+m_b r_b^2$
[6] $k= \omega^2 I$
[7] $c=2\omega\zeta$

Table 1. Constants in 9 m and 25 m models.

25m Blade	Rigid Body	Lumped Mass
Maximum Hydraulic Force (kN)	-58.9	-130.7
Minimum Hydraulic Force (kN)	-203.6	-131.9
Amplitude of Force Curve	144.7	1.2
Actuator Stroke (cm)	±11.2	±0.4

Table 2. Comparison of hydraulic forces and stroke from rigid body and base excitation models of NWTC test-stand and 25m blade. Negative numbers indicate that the actuator is pulling.

Model Outputs

As shown in Table 2, the forces required in the lumped mass model are considerably lower than those in the rigid body model. Additionally, the amplitude, or ½ the difference between the maximum and minimum hydraulic force, is reduced by more than a factor of 100. This reduction of forces in the lumped mass model is a result of the blade oscillating at its natural frequency. As shown in Figure 3, the moment due to the elasticity of the blade and the moment due to the rotational inertia of the blade cancel.

The moment due to the rotational inertia of the test-stand is also reduced. Because the base excitation model includes the elastic properties of the blade, the test-stand displacement (O_h, Equation 3) required to produce a displacement on the blade (B) is lowered from 2° to 0.08°. This small angular displacement appears unintuitive. To ensure that the angular displacement is reasonable, displacements from an ongoing 9 m blade fatigue test were measured (Table 3). The 0.06° displacement at the center of gravity validates the result that only very small displacements are required to produce desired tip displacements and corresponding strains. The small angular

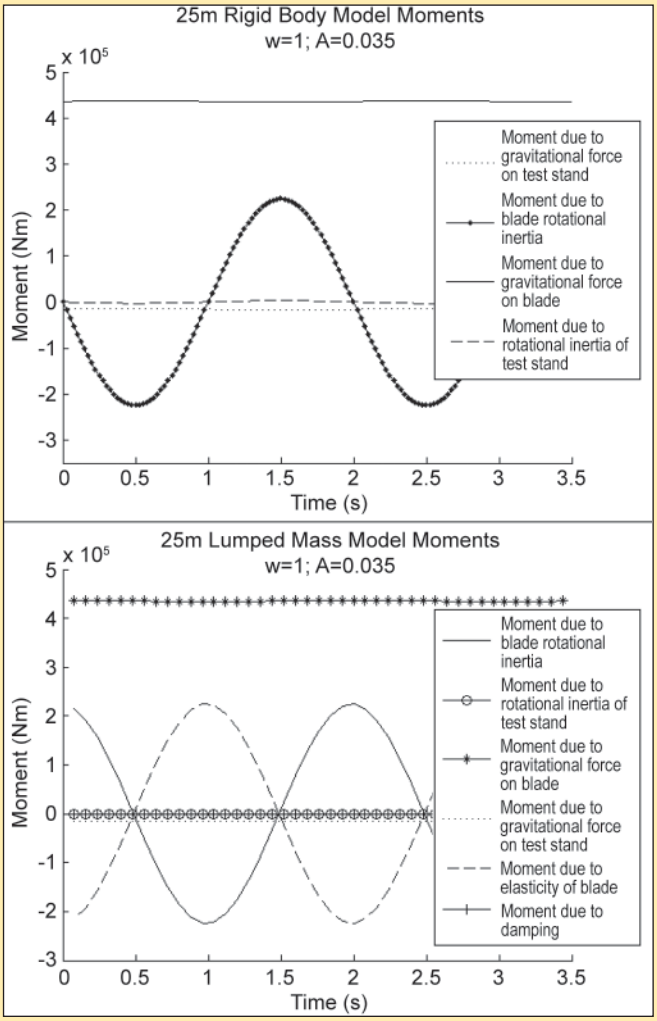

Figure 3. Comparison of rigid body and base excitation models for hypothetical 25 m blade. Note that in the base excitation model, the moment due to the rotational inertia of the test stand and moment due to damping overlap along the x-axis.

displacement translates into a short required stroke from the forcing hydraulic actuators (Table 2).

The elastic lumped-mass model is also used to compute forces for an experimental 9 m blade (Figure 3, Table 4). In this case, the magnitude of the required force is reduced because the moment due to the gravitational force on the blade is significantly reduced. The force is also reduced because the blade and test stand are in close to static equilibrium. In order to reduce the loads required by a 25 m blade, the test stand was also modeled with a large counterweight. The counterweight addition significantly lowers the loads required from the hydraulic actuator (Table 5).

	9m TX Blade Test	Model
Displacement at CG	± 0.060°	± 2.0°
Displacement at root		±0.078
Displacement at Tip	± 1.3°	± 2.0°

Table 3. Comparison of displacements on NWTC test-stand from base excitation model and 9 m TX blade fatigue test.

9m TX Blade	Rigid Body	Lumped Mass
Maximum Hydraulic Force (kN)	4.38	1.64
Minimum Hydraulic Force (kN)	-1.22	1.59
Amplitude of Force Curve	2.8	0.025

Table 4. Comparison of hydraulic forces from rigid body and base excitation models of NWTC test-stand and 9m blade. Negative numbers indicate that the actuator is pulling.

25m blade	Base Excitation	Statically Balanced Base Excita-
Maximum Hydraulic Force (kN)	-130.7	1.1
Minimum Hydraulic Force (kN)	-131.9	-1.1
Amplitude of Force Curve (kN)	1.2	1.1

Table 5. Comparison of hydraulic forces on NWTC test-stand from base excitation and statically balanced base excitation models.

Component Considerations

Hydraulic Actuators

The hydraulic actuators should be sized to exceed the maximum loads imposed by base oscillation of a 25 m blade. For a successful certification test, actuators must supply a smooth sinusoidal input force; double ended actuators ensure this input force. Additionally, actuators should be oversized to ensure a sufficient margin of safety to avoid damage. Fatigue rated cylinders should be used for the longevity of the system. The prototype test-stand will use 14.7 kN (3.3 kip) fatigue rated actuators already owned by the laboratory.

Load Cell

A load cell is placed in line with the hydraulic actuators to measure the supplied force; however, the rigidity of the stand cannot be compromised. A stand which is not rigid will distort test results. Lash should be removed from the system using spiral washers or another like system.

Bearings

Unlike the UREX, the MOFO requires the test-stand to oscillate. Radial loads dominate the test-stand, but axial loads are also present as a result of twist bending in blades and possibly dual axis testing; bearings must carry both loads. The bearings chosen must also avoid lubrication issues with repetitive small angular displacements.

Safety System

Although displacements on the test-stand are small, the center of gravity of the system with large blades lies outboard of the test-

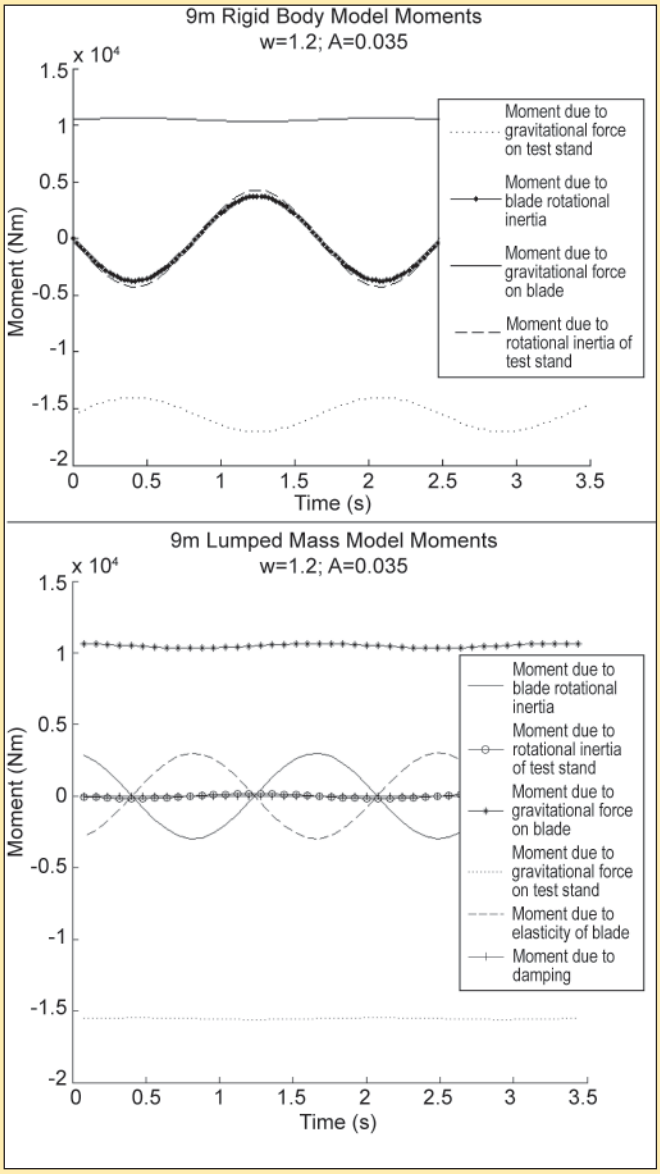

Figure 4. Comparison of rigid body and base excitation models for 9 m blade. Note that in the base excitation model, the moment due to the rotational inertia of the test stand and moment due to damping overlap along the x-axis.

stand. If the hydraulic pressure is cut, or if user-error occurs, the test-stand will rotate forward until the blade contacts the floor or rotate backward until the blade either contacts the ceiling or the actuator retracts enough to hit the cushion. This may damage the blade and poses a serious safety risk. Using the hydraulic actuator's cushion, dampers on the test stand, and blade straps should be incorporated to the stand's design.

Blade Moment Distributions

For simplicity and design characterization, the above modeling assumes that the blade has a constant bending moment distribution. Real blades, however, have complex bending moment distributions based on the individual design, materials, and construction. With previous blade mounted testing designs, loads have been applied at the center of mass of the test stand. Using the MOFO, however, loads will be applied at the root of the blade. A basic model comparing the load application showed differences in internal bending moment distributions. This finding has implications for the individual blade testing but does not affect the overall loads and characterization of the test stand.

Conclusions and Future Work

Through the preceding modeling and conceptual design process, it has been concluded that creating a 25 m prototype Mobile Oscillatory Fatigue Operator (MOFO) from a current NWTC test-stand will be able to generate loads and displacements required to replace the current UREX testing system. The MOFO will simplify testing as a universal test stand. Two dynamic models were completed for 9 m and 25 m blades to size hydraulics. For the project to proceed, the dynamic model should be validated. This can be achieved through further dynamic modeling using software such as SIMPACK or ADAMS or by completing a fatigue test on the 9 m TX blade and comparing the results. Further modeling should also be completed to determine the moment distribution within blades using the new test methodology.

Acknowledgements

This research was conducted at the National Wind Technology Center at the National Renewable Energy Laboratory through the Office of Science's Science Undergraduate Laboratory Internship program. I would like to thank my mentor, Jason Cotrell as well as Scott Hughes, Jeroen van Dam, Gunjit Bir, Sandy Butterfield, Trey Riddle, Scott Lambert, Peter Kasell and Francisco Oyague for their assistance. I would also like to thank the Department of Energy's Office of Science and the Office of Education at the National Renewable Energy Laboratory for supporting such a rewarding internship program.

Appendix A

A.1 Derivation of Rigid Body Model

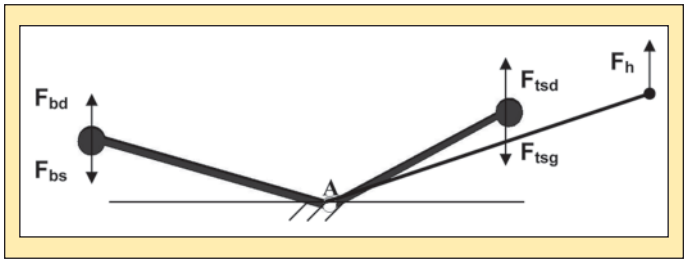

The torques are summed about the pivot, A.

$\Sigma\tau_A=\tau_{ts}-\tau_b+\tau_{Fh}$

Each torque can be written in terms of its dependent terms.

It is assumed that the actuator acts only in the vertical direction.

$\tau_{Fh}=F_h(t)r_h=F_h(t)l_h\cos\theta_{h0}$

The test stand and blade perturbations are driven at the natural frequency of the blade, ω and desired amplitude, *B*.

$\theta=B\sin(\omega\tau)$

$\theta=B\omega\cos(\omega\tau)$

$\theta=B\omega^2\sin(\omega\tau)$

The resulting torque from the blade can be split into two a static torque due to gravity and a dynamic torque due to rotational inertia, as well as an initial angle θ_{b0} and the perturbation, θ.

$\tau_b=\tau_{b\text{-}static}+\tau_{b\text{-}dynamic}$

$\tau_{b\text{-}static}=-m_b g r_b=-m_b g l_b\cos(\theta_b)=-m_b g l_b\cos(\theta_{b0}-\theta)$

$\tau_{b\text{-}dynamic}=\theta_b I_b=-\theta I_b$

The negative sign results from the blade being fastened on the opposite side of the pivot point as the actuators.

The same procedure is followed for the torque from the test stand.

$\tau_{ts}=\tau_{ts\text{-}static}+\tau_{ts\text{-}dynamic}$

$\tau_{ts\text{-}static}=-m_{ts} g r_{ts}=-m_{ts} g l_{ts}\cos(\theta_{ts})=-m_{ts} g l_{ts}\cos(\theta_{ts0}+\theta)$

$\tau_{ts\text{-}dynamic}=\theta_{ts} I_{ts}=\ddot{\theta} I_{ts}$

Substituting back in terms yields

$$F_h(t)=\frac{-1}{l_h\cos(\theta_{h0})}(m_b g l_b\cos(\theta_{b0}-\theta)+\ddot{\theta} I_b-m_{ts} g l_{ts}\cos(\theta_{ts0}+\theta)+\ddot{\theta} I_{ts})$$

A.2 Derivation of Lumped Mass Model

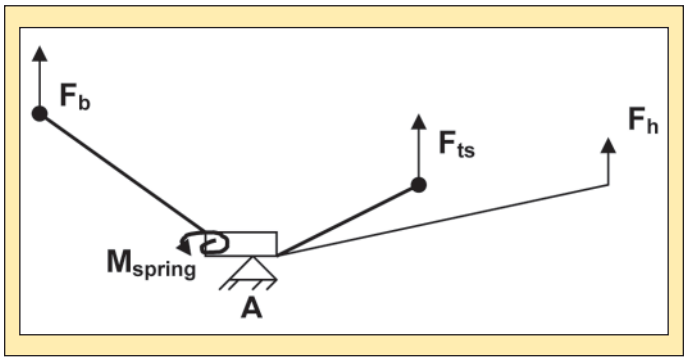

The same governing equation can be derived for the lumped mass model as the rigid body model with the addition of a spring and a damping term.

$$F_h(t)=\frac{-1}{l_h\cos\theta_{h0}}(m_b\,gl_b\cos(\theta_{b0}+\theta_b)-\ddot{\theta}_b I_b-m_{ts}\,gl_{ts}\cos(\theta_{ts0}+\theta_{ts})$$
$$+\ddot{\theta}_{ts}I_{ts}-k(\theta_b-\theta_{ts})-c(\dot{\theta}_b-\dot{\theta}_{ts}))$$

However, the input and response functions, θ_b and θ_{ts}, are no longer governed by the simple $\theta=\sin(\omega t)$. The governing equation describing the base excitation vibration of the blade with a given sinusoidal input is a second order linear differential equation[1].

$$\theta_{ts}=Y\sin(\omega t)$$
$$I\ddot{\theta}_b+c(\dot{\theta}_b-\dot{\theta}_{Fb})+k(\theta_b-\theta_{ts})=0$$

The solution for the response function, θ_b, is dependent only the system damping when driven at the blade's natural frequency. When the damping coefficient is small ($\varsigma \approx< 0.05$), the blade trails the test stand approximately 90° out of phase.

$$\theta_b=\omega Y\left[\frac{\omega^2+(2\varsigma\omega)^2}{(2\varsigma\omega^2)^2}\right]^{\frac{1}{2}}\cos(\omega t-\frac{\pi}{2}-\arctan(\frac{1}{2\varsigma}))$$
$$=Y\left[\frac{1+(2\varsigma)^2}{(2\varsigma)^2}\right]^{\frac{1}{2}}\cos(\omega t-\frac{\pi}{2}-\arctan(\frac{1}{2\varsigma}))$$

The coefficient, Y, is unknown; however, the amplitude of the blade displacement is driven. The desired amplitude B is known. From the above equation, the amplitude of the input function Y can be solved.

$$Y=B\left[\frac{\omega^2+(2\varsigma\omega)^2}{(2\varsigma\omega^2)^2}\right]^{-\frac{1}{2}}=B\left[\frac{1+(2\varsigma)^2}{(2\varsigma)^2}\right]^{-\frac{1}{2}}$$

The governing equation is reduced to one unknown, $F_h(t)$.

$$F_h(t)=\frac{-1}{l_h\cos(\theta_{h0})}(m_b\,gl_b\cos(\theta_{b0}+B\cos(\omega t-\frac{\pi}{2}-\arctan(\frac{1}{2\varsigma}))$$
$$+B\cos(\omega t-\frac{\pi}{2}-\arctan(\frac{1}{2\varsigma}))I_b$$
$$-m_{ts}\,gl_{ts}\cos(\theta_{ts0}+B\left[\frac{1+(2\varsigma)^2}{(2\varsigma)^2}\right]^{-\frac{1}{2}}\sin(\omega t)-\omega^2B\left[\frac{1+(2\varsigma)^2}{(2\varsigma)^2}\right]^{-\frac{1}{2}}\sin(\omega t)I_{ts}$$
$$-kB(\cos(\omega t-\frac{\pi}{2}-\arctan(\frac{1}{2\varsigma}))-B\left[\frac{1+(2\varsigma)^2}{(2\varsigma)^2}\right]^{-\frac{1}{2}}\sin(\omega t))$$
$$+cB\omega(\sin(\omega t-\frac{\pi}{2}-\arctan(\frac{1}{2\varsigma}))-\left[\frac{1+(2\varsigma)^2}{(2\varsigma)^2}\right]^{-\frac{1}{2}}\sin(\omega t)$$

The value of k is calculated from the known natural frequency of the blade and rotational moment of inertia.

$$k=\omega^2 I_b$$

The blade rotational inertia and spring term dependent on θ_b cancel.

$$F_h(t)=\frac{-1}{l_h\cos(\theta_{h0})}[m_b\,gl_b\cos(\theta_{b0}+B\cos(\omega t-\frac{\pi}{2}-\arctan(\frac{1}{2\varsigma}))+$$
$$-m_{ts}\,gl_{ts}\cos(\theta_{ts0}+B\left[\frac{1+(2\varsigma)^2}{(2\varsigma)^2}\right]^{-\frac{1}{2}}\sin(\omega t))$$
$$-\omega^2B\left[\frac{1+(2\varsigma)^2}{(2\varsigma)^2}\right]^{-\frac{1}{2}}\sin(\omega t)I_{ts}+cB\omega(\sin(\omega t-\frac{\pi}{2}-\arctan(\frac{1}{2\varsigma}))]$$

If the test stand is balanced, the static terms also cancel, leaving a simplified equation.

$$F_h(t)=\frac{-1}{l_h\cos(\theta_{h0})}[-\omega^2B\left[\frac{1+(2\varsigma)^2}{(2\varsigma)^2}\right]^{-\frac{1}{2}}\sin(\omega t)I_{ts}$$
$$+cB\omega(\sin(\omega t-\frac{\pi}{2}-\arctan(\frac{1}{2\varsigma}))$$
$$-\left[\frac{1+(2\varsigma)^2}{(2\varsigma)^2}\right]^{-\frac{1}{2}}\sin(\omega t))+kB(-B\left[\frac{1+(2\varsigma)^2}{(2\varsigma)^2}\right]^{-\frac{1}{2}}\sin(\omega t))]$$

1 Daniel J Inman, *Engineering Vibration*. Prentice-Hall Inc. Englewood Cliffs, NJ: 1994.